Planta (2008) 228:823–838
DOI 10.1007/s00425-008-0785-2

OpenAccess

ORIGINAL ARTICLE

AtCSLD2 is an integral Golgi membrane protein with its N-terminus facing the cytosol

Weiqing Zeng · Kenneth Keegstra

Received: 5 May 2008 / Accepted: 4 July 2008 / Published online: 19 July 2008

Abstract Cellulose synthase-like proteins in the D family share high levels of sequence identity with the cellulose synthase proteins and also contain the processive β-glycosyltransferase motifs conserved among all members of the cellulose synthase superfamily. Consequently, it has been hypothesized that members of the D family function as either cellulose synthases or glycan synthases involved in the formation of matrix polysaccharides. As a prelude to understanding the function of proteins in the D family, we sought to determine where they are located in the cell. A polyclonal antibody against a peptide located at the N-terminus of the *Arabidopsis* D2 cellulose synthase-like protein was generated and purified. After resolving Golgi vesicles from plasma membranes using endomembrane purification techniques including two-phase partitioning and sucrose density gradient centrifugation, we used antibodies against known proteins and marker enzyme assays to characterize the various membrane preparations. The *Arabidopsis* cellulose synthase-like D2 protein was found mostly in a fraction that was enriched with Golgi membranes. In addition, versions of the *Arabidopsis* cellulose synthase-like D2 proteins tagged with a green fluorescent protein was observed to co-localize with a DsRed-tagged Golgi marker protein, the rat alpha-2,6-sialyltransferase. Therefore, we postulate that the majority of *Arabidopsis* cellulose synthase-like D proteins, under our experimental conditions, are likely located at the Golgi membranes. Furthermore, protease digestion of Golgi-rich vesicles revealed almost complete loss of reaction with the antibodies, even without detergent treatment of the Golgi vesicles. Therefore, the N-terminus of the *Arabidopsis* cellulose synthase-like D2 protein likely faces the cytosol. Combining this observation with the transmembrane domain predictions, we postulate that the large hydrophilic domain of this protein also faces the cytosol.

Keywords *Arabidopsis* · AtCSLD2 · Cell wall · Golgi · Localization · Topology

Abbreviations

CESA	Cellulose synthase
CSLD	Cellulose synthase-like protein D
ER	Endoplasmic reticulum
FUTase	Fucosyltransferase
GS II	β-Glucan synthase II
PGA	Polygalacturonic acid
PMA2	Plasma membrane H^+-ATPase 2
PVC	Pre-vacuolar compartment
ST	Alpha-2,6-sialyltransferase
TGN	*Trans*-Golgi network
XT1	Xylosyltransferase 1
XyG	Xyloglucan

W. Zeng · K. Keegstra (✉)
DOE-Plant Research Laboratory, Michigan State University,
Room 110, Plant Biology Building, East Lansing, MI 48824, USA
e-mail: keegstra@msu.edu

W. Zeng
e-mail: zengweiq@msu.edu

W. Zeng
Cell and Molecular Biology Program,
Michigan State University, East Lansing, MI 48824, USA

K. Keegstra
Department of Biochemistry and Molecular Biology,
Michigan State University, East Lansing, MI 48824, USA

K. Keegstra
Department of Plant Biology, Michigan State University,
East Lansing, MI 48824, USA

Introduction

CSLD proteins constitute a group belonging to the cellulose synthase superfamily of proteins. Members of this group have the highest sequence similarity to CESA proteins within the cellulose synthase superfamily, showing sequence identities of 40–45% (Richmond and Somerville 2001). CSLD proteins are also similar in size to CESA proteins and have a similar number and organization of predicted transmembrane domains (Richmond and Somerville 2001). Moreover, CSLD and CESA proteins share structural features that may be indicative of processive glycosyltransferases (Saxena et al. 1995), such as the D,D,D,Q××RW motif proposed to define the nucleotide-sugar binding domain and the catalytic site (Richmond and Somerville 2000) of the cellulose synthases. Both CSLD and CESA proteins belong to family 2 of inverting nucleotide-diphospho-sugar glycosyltransferases, which synthesize polysaccharides containing repeating β-glycosyl units (Campbell et al. 1997; Richmond and Somerville 2001).

Pinpointing the localization of CSLD proteins may shine some light on their putative functions, because efforts to identify their biochemical function through heterologous expression and enzymatic activity assays have not been successful to date (Liepman et al. 2005). If CSLD proteins are truly cellulose synthase isoforms, they might exhibit a localization pattern similar to CESA. If CSLD proteins are involved in the biosynthesis of other matrix polysaccharides, they might be expected to have a different localization pattern than CESA proteins and reside on the Golgi membranes, as other matrix polysaccharides are thought to be synthesized in Golgi complexes and then transported to the cell surface via membrane-bound vesicles for incorporation into the wall matrix (Delmer and Stone 1988).

AtCSLD3 protein was localized to the endoplasmic reticulum (ER) when Favery et al. transiently expressed a C-terminal tagged AtCSLD3-GFP fusion protein in *Nicotiana benthamiana* leaf cells (Favery et al. 2001). This ER localization of AtCSLD3 protein was seen again by Bernal et al. when a GFP tag was placed at the C-terminus of AtCSLD3 or AtCSLD5 (Bernal et al. 2007). However, when the GFP tag was placed at the N-terminus of AtCSLD5 or AtCSLD3, both the fusion proteins were localized to the Golgi apparatus (Bernal et al. 2007). Furthermore, a proteomic approach using the isotope-tagging technique to localize organelle proteins also identified AtCSLD3 in the Golgi apparatus (Dunkley et al. 2006). To further investigate the localization of AtCSLD proteins, we used a biochemical approach to fractionate cellular organelles and localized AtCSLD2 proteins to the Golgi fraction by means of an AtCSLD2-specific antibody. We substituted the predicted non-transmembrane hydrophilic domain of AtCSLD2 with a GFP tag and visualized the fusion proteins in the Golgi apparatus as well.

The current working model predicts that Golgi-localized glycosyltransferases involved in wall matrix polysaccharide biosynthesis catalyze their specific reactions inside the Golgi lumen, with their catalytic domains facing the lumen and their sugar nucleotide substrates being transported into the Golgi from the cytosol (Northcote and Pickett-Heaps 1966; Zhang and Staehelin 1992; Norambuena et al. 2002). More recent topology studies of such glycosyltransferases include the protection of enzyme activities from protease treatment by the Golgi membranes, for the α-1, 4-galacturonosyltransferase involved in the biosynthesis of homogalacturonan (Sterling et al. 2001), and the β-1, 4-galactosyltransferase involved in the synthesis of β-1, 4-galactan side chains in rhamnogalacturonan I (Geshi et al. 2004). On the other hand, the maize mixed linkage (1–3), (1–4)-β-D-glucan synthase was found to be sensitive to pretreatments of Golgi membranes with proteinase K (Urbanowicz et al. 2004). Therefore, the topology of (1–3), (1–4)-β-D-glucan synthase was proposed to be more closely related to the cellulose synthase than to non-cellulosic glucan synthase or glycosyltransferases (Urbanowicz et al. 2004). Generally, cellulose synthases located at the plasma membrane are predicted to have their active site facing the cytoplasmic side of the membrane (Kimura et al. 1999) and use sugar nucleotide substrates from the cytosol, incorporating them into cellulose on the other side of the plasma membrane.

Here, using similar proteinase protection assays, we present evidence that the N-terminus of AtCSLD2 protein is not protected by the un-solubilized Golgi membranes and therefore must be facing the cytosol. Combining this observation with predictions regarding the topology of AtCSLD2 in the membrane leads to the hypothesis that its putative large hydrophilic loop also faces the cytosol.

Materials and methods

Plant materials

Arabidopsis plants were grown under non-sterile hydroponic conditions (Gibeaut et al. 1997) in growth chambers in an 18 h/6 h light/dark cycle and light/dark temperature of 22°C/20°C. *Arabidopsis* (ecotype Columbia) embryonic suspension cell line T87-C33 (Axelos et al. 1992) was maintained in the dark at 25°C in suspension culture medium (20 g L^{-1} sucrose, 4.3 g L^{-1} Murashige–Skoog salts [GIBCO-BRL], 0.5 g L^{-1} MES, 0.1 g L^{-1} myo-inositol, 1 mg L^{-1} thiamine-HCl, 1 μM 2,4-D, and 1 mM K_2HPO_4, pH 5.7).

Preparation of total protein fraction and microsomal membranes from *Arabidopsis* plants

Tissues from 5-week-old hydroponically grown *Arabidopsis* plants were ground in liquid nitrogen and resuspended in extraction buffer A (150 mM Tris HCl at pH 6.8, 3% SDS, 7.5% 2-mercaptoethanol) at 2 ml g^{-1} fresh weight. The extracts were boiled for 15 min and centrifuged for 15 min at 10,000*g*. The supernatants were saved as total protein fractions.

For microsomal membrane preparations, each 20-g sample of tissue from 5-week-old *Arabidopsis* plants was cut into small pieces with a Comfort Food Chopper (Zyliss, Switzerland) and ground with mortar and pestle on ice in 40 ml extraction buffer B (50 mM Hepes KOH, pH 6.5, 10 mM potassium acetate, 2.5 mM EDTA, 0.4 M sucrose, 1 mM DTT, 0.2 mM PMSF, 1% Protease Inhibitors [Sigma]). After passage through a double layer of miracloth, extracts were centrifuged at 10,000*g* for 10 min at 4°C. The pellet was resuspended in buffer B as the P10 fraction. The supernatant S10 fraction was subjected to further centrifugation at 100,000*g* for 1 h at 4°C. The supernatant from this step was the S100 fraction, and the pellet was resuspended in extraction buffer B, usually of one-tenth of the starting volume, as the P100 fraction.

Preparation of S10 protein fraction and microsomal membranes from *Arabidopsis* cell suspension cultures

Arabidopsis suspension cells, cultured for 4 to 5 days were collected on miracloth using vacuum filtration. Usually, 20 g of cells were suspended at a concentration of 1/3 g ml^{-1} of extraction buffer C (50 mM Hepes KOH, pH 6.5, 2 mM EDTA, 15% sucrose, 1 mM DTT, 0.2 mM PMSF, 1% Protease Inhibitors [Sigma]). Cells were disrupted in a blender with short bursts of 10 s for a total of 1 min on ice. Cell lysate was filtered through a double layer of miracloth and subjected to centrifugation at 10,000*g* for 10 min at 4°C. The supernatant was saved as the S10 protein fraction, and the pellet was discarded. The supernatant solution was then centrifuged at 100,000*g* for 1 h at 4°C to yield the S100 fraction, and a membrane pellet was resuspended in extraction buffer C at one-tenth of the starting volume and labeled as the P100 fraction.

Solubilization of microsomal membrane proteins

P100 microsomal fractions were isolated from either 5-week-old hydroponically grown *Arabidopsis* above-ground tissues or from 4- to 5-day-old *Arabidopsis* suspension-cultured cells. Equal amounts of P100 microsomal protein were resuspended in the same amount of extraction buffer C and incubated with equal volume of the same buffer containing 4 M Urea, 2 M NaCl, 0.2 M Na_2CO_3, 0.4% Triton X-100, 0.4% SDS or buffer C alone for 30 min on ice. After treatment, all solutions were centrifuged at 100,000*g* again for 1 h at 4°C. Supernatants were saved and the pellets were resuspended in the same volume of buffer C. Equal volumes of each fraction were used for SDS-PAGE and immunoblotting.

Sucrose density gradient fractionation of microsomal membranes

The S10 protein fraction isolated from *Arabidopsis* suspension-cultured cells was subjected to a two-step sequential sucrose gradient fractionation. The first sucrose gradient was made in an SW28 centrifuge tube with two layers of 10 ml of buffer C, containing 50 and 15% of sucrose, respectively. The S10 protein fraction was loaded on top of the gradient and subjected to a centrifugation of 100,000*g* for 1 h at 4°C. The interface between the two sucrose solutions, which was about 2 ml in volume, was recovered and diluted with the buffer C lacking sucrose until the sucrose concentration reached between 25 and 30%. This diluted interface was used for the second centrifugation step. The second sucrose gradient, made in an SW40 centrifuge tube, was linear and contained 30–50% sucrose in buffer C. About 2.5 ml of the diluted interface from the first step was laid on top of the linear gradient and centrifuged at 100,000*g* for 3 h at 4°C. Fractions of 800 µl each were collected with an Auto Densi-Flow fractionator (Labconco). Sucrose concentrations were determined with a refractometer (American Optical Corporation, Buffalo, NY).

Two-phase partitioning

The two-phase partitioning method for the purification of plasma membranes was modified from a previous protocol (Larsson et al. 1987). The crude microsomal membranes from suspension-cultured *Arabidopsis* cells (P100 pellet) were resuspended in buffer D (0.33 M sucrose, 3 mM KCl, 5 mM potassium phosphate at pH 7.8, Protease Inhibitors [1:100, Sigma]) in one-tenth of the starting volume of the S10 fraction. For every 3 g of this microsome solution, 9 g of buffer E (buffer D plus 8.4% Dextran T500 and 8.4% PEG 3350) was added to make a final concentration of 6.3% of both Dextran and PEG. The tubes were inverted 30 times for mixing, and the samples were centrifuged at 1,500*g* for 5 min at 4°C in a swinging bucket rotor. The upper phase was collected as the U1 fraction, and the lower phase as the L1 fraction. Buffer F (buffer D plus 6.3% Dextran T500 and 6.3% PEG 3350) was prepared fresh and allowed to sit overnight at 4°C to separate the two phases. The U1 fraction was further extracted twice with equal volumes of the lower phase from buffer F to produce phases U2, L2′, U3, and L3′ sequentially. The L1 fraction was also

further extracted twice with equal volumes of the upper phase from buffer F, to produce the U2′, L2, U3′ and L3 phases. Equal volumes of each phase or equal amounts of protein from each phase were used for SDS-PAGE and enzyme activity assays. Protein concentration was determined with a Micro BCA kit (Pierce, Rockford, IL, USA).

Preparation of Golgi-rich microsomal membrane fractions

The centrifugation procedure developed by Buckeridge et al. (1999) for maize was adopted for use with *Arabidopsis*. The S10 protein fraction was prepared from 4- to 5-day-old suspension-cultured cells, as described for other applications, except that buffer G (84% sucrose [w/v], 20 mM Hepes KOH, pH 7.0, 20 mM KCl, 5 mM EDTA, 5 mM EGTA, 10 mM DTT, Protease Inhibitors [1:100, Sigma]) was used. The sucrose concentration in the S10 fraction was determined with a refractometer (American Optical Corporation, Buffalo, NY) and adjusted to around 40% (37–45%) using buffer G containing no sucrose or 84% sucrose, depending on the need. Sucrose gradient was made in gradient buffer H containing 20 mM Hepes KCl, pH 7.0, Protease Inhibitors (1:100, Sigma), and various concentrations of sucrose.

To make a gradient, 10 ml of S10 total protein with adjusted sucrose concentration was laid on top of 5 ml of buffer H containing 50% (w/v) sucrose in an SW28 centrifuge tube. On top of the sample, we added sequentially buffer H: 8 ml with 34% (w/v) sucrose, 8 ml of 25% (w/v) sucrose, and 7 ml of 18% (w/v) sucrose. About 2 ml of buffer H containing 9.5% (w/v) sucrose was used to fill the tube completely. This filled tube was centrifuged at 100,000*g* for 1.5 to 3 h at 4°C. After centrifugation, the interfaces between layers were collected and designated as fraction 1, 2, 3, 4, or 5 from the top to the bottom of the gradient. According to the original protocol (Buckeridge et al. 1999), those five fractions are enriched with tonoplast, ER, Golgi, mitochondria, and plasma membrane, specifically. Here, only fractions 3, 4, and 5 were further characterized and used for the localization studies. These three fractions were diluted in buffer H to sucrose content below 15% and centrifuged again at 100,000*g* for 50 min. The pellet fractions were resuspended in buffer H without sucrose. Protein concentrations were determined using the Micro BCA kit from PIERCE (Rockford, IL).

Expression of polypeptides P2 and P3 in *E. coli* cells

The DNA sequence encoding the first 272 amino acids of AtCSLD2 (fragment P2) was amplified from *Arabidopsis* genomic DNA using primers *KEE919* (5′-CCTACATATG GCATCTAATAAG-3′) and *KEE921* (5′-TCATGAATT CTTGGGCCTCCAT-3′). The DNA sequence encoding the first 188 amino acids of AtCSLD3 (fragment P3) was amplified from *Arabidopsis* genomic DNA using primers *KEE920* (5′-TTAGCATATGGCGTCTAATAAT-3′) and *KEE922* (5′-CTGCTTGTTGTTCTCGAGCAAA-3′). Purified PCR products were inserted into pET28a via *Nde*I and *Eco*RI for the DNA fragment encoding P2, and via *Nde*I and *Xho*I for the DNA fragment encoding P3. The identities of constructs encoding peptides P2 and P3 were confirmed by restriction digestion and sequencing. Peptide fragments P2 and P3 were expressed in *E. coli* BL21 (DE3) cells according to the manufacturer's guidelines (pET System Manual, Novagen, Madison, WI). Total soluble proteins were extracted from 100 ml of *E. coli* cultures expressing each construct after 4 h induction with IPTG.

Generation and purification of polyclonal antibodies directed against AtCSLD2

AtCSLD2-specific peptide IQEPGRPPAGHSVKFAQ(C), corresponding to a region near the N-terminus (aa20–aa36), was synthesized and conjugated with keyhole limpet hemacyanin (KLH) for polyclonal antibody production in rabbits (Alpha Diagnostic International Inc., San Antonio, TX, USA). The polyclonal antibodies were affinity purified with the same peptide immobilized on the SulfoLink coupling gel (PIERCE, Rockford, IL, USA) according to the manufacturer's directions.

SDS-PAGE and immunoblotting

All SDS-PAGE and immunoblotting procedures followed standard protocols (Harlow and Lane 1988). Antibody against PMA2 (Morsomme et al. 1998), a *Nicotiana plumbaginifolia* plasma membrane H^+-ATPase, was a gift from Dr. Marc Boutry (Université Catholique de Louvain, Louvain-la-Neuve, Belgium). Antibodies against TGN marker SYP61 (Sanderfoot et al. 2000), PVC marker SYP21 (Sanderfoot et al. 1999), TGN-PVC marker ELP (Ahmed et al. 1997) and ER marker SEC12 (Bar-Peled and Raikhel 1997) were gifts from Dr. Natasha Raikhel (University of California, Riverside). Antibody against alternative oxidase, a gift from the late Dr. Lee McIntosh (Michigan State University), is a monoclonal antibody against the *Sauromatum guttatum* alternative oxidase located in mitochondria (Elthon et al. 1988). Rabbit antibody against XT1 was generated by Dr. Ahmed Faik (unpublished data) using a 17-kD fragment of the *Arabidopsis* XT1 protein that was expressed in *E. coli.*

Marker enzyme assays

The assay for β-glucan synthase II (callose synthase, GS II) activity was modified from existing protocols (White et al.

1993; Konishi et al. 2001). The reaction mixture contained 50 mM Hepes KOH, pH 7.0, 1 mM UDP-Glc, 5 mM $CaCl_2$, 4.36 μM UDP-[^{14}C]Glc (305.9 mCi/mmol). Reactions were carried out at room temperature for 45 min. XyG carrier (5 μl of a 1% solution) was added to each reaction before 750 μl of 70% ethanol was added to stop the reactions. Reaction products were precipitated at room temperature for 30 min and washed three times with 70% ethanol by mixing, followed by centrifugation at 12,000*g* for 5 min. The pellet was then air dried and resuspended in 200 μl H_2O for scintillation counting.

For XyG FUTase activity assays, microsomal membranes were solubilized with 1% Triton X-100 for 15 min on ice immediately before enzyme assays, unless solubilization of samples was not required. Assay reactions were carried out in volumes of 50 μl, including 10 μl of solubilized P100 membranes (9 μl P100 sample plus 1 μl 10% Triton X-100), 20 μl of 2.5× reaction buffer (100 mM HEPES KOH, pH 6.8, 0.5 M sucrose, 2.5 mM DTT, 2.5 mM $MgCl_2$), 10 μl of 1% tamarind seed XyG and 2.5 μl (diluted to 10 μl with H_2O before use) of GDP ^{14}C-fucose (10 μCi/ml and 271 mCi/mmol) (NEN Life Science Products, Inc.). Reactions were carried out at room temperature and stopped by the addition of 1 ml of 70% ethanol. Products of the enzyme assays were precipitated at 4°C or room temperature for at least 2 h and washed three times with 70% ethanol. After the last washing, the pellet was briefly air dried and resuspended in 200 μl H_2O for scintillation counting.

Proteinase K protection assay

Membrane vesicles enriched in Golgi were purified from 20 g of suspension-cultured cells according to the protocol described above, and resuspended in 0.6 ml of buffer H without the addition of protease inhibitors. Equal amounts (90 μl) of purified Golgi-rich vesicles were then incubated with 0, 200, and 400 μg/ml proteinase K (Roche, Penzberg, Germany) with or without the addition of 1% Triton X-100 for 30 min at 25°C. The reactions were stopped by the addition of 5 μl of 200 mM PMSF and left on ice. From each reaction, a 9-μl aliquot was used for a XyG FUTase assay and a 30-μl aliquot was analyzed by SDS-PAGE and immunoblotting.

Construction and localization of AtCSLD2-GFP

A DNA fragment *cD2tmd* encoding AtCSLD2 peptide from aa890 to aa1145 (end) containing the predicted C-terminal transmembrane domains was amplified through PCR reaction using primers *D2d* (upstream, 5′ TTTTCACTAGT AACAACGCTCTTC 3′, *Spe*I) and *D2b* (downstream, 5′ TCAACGGTACCTGGAAAACTGAA 3′, *Kpn*I). This fragment was inserted into GFP expression vector GFPc (a gift from Dr. Shuocheng Zhang, Michigan State University) downstream of the encoded GFP protein via *Spe*I and *Kpn*I to make the construct *GFP-cD2tmd*. A DNA fragment *nD2tmd* encoding AtCSLD2 peptide from aa1 to aa380 containing the predicted N-terminal transmembrane domains was amplified through RT-PCR reaction using primers *D2e* (upstream, 5′ AAGTTGGATCCTAACTA TGGCAT 3′, *Bam*HI) and *D2f* (downstream, 5′ TCCTTGG ATCCTGAACTCGCCAGAACCAGCAGCGGAGCCAG CGGAACCGGTGGCACGATTAATCGGGCATAGCTT 3′, *Bam*HI). This fragment was inserted into construct *GFP-cD2tmd* in front of the encoded GFP protein via *Bam*HI, to make the final construct *nD2tmd-GFP-cD2tmd*.

Plasmid nD2tmd-GFPc-cD2tmd and ST-DsRed (gift from Dr. Federica Brandizzi, Michigan State University), or plasmid GFPc plus ST-DsRed were introduced into onion epidermal cells using biolistic bombardment according to Zhang et al. (2001). After being kept in the dark for 16–20 h, the onion peels were observed by means of an upright laser-scanning confocal microscope (Zeiss LsM510 META; Zeiss) according to Hanton et al. (2007).

Results

Expression of *AtCSLD* genes

To investigate the localization of proteins encoded by *AtCSLD* genes, we chose to start with *AtCSLD2* and *AtCSLD3* because of their expression patterns. These two genes showed higher levels of expression than other members of the *AtCSLD* subfamily and their expression patterns were similar to each other based on analysis of the EST database from the GenBank and MPSS database (http://mpss.udel.edu/at/). Furthermore, RT-PCR reactions using RNAs isolated from various tissues of *Arabidopsis* confirmed the conclusion that *AtCSLD2* and *-D3* are expressed at higher levels than other *AtCSLD* genes and their expression patterns were similar to each other (Zeng 2004).

Generation, purification, and characterization of antibodies against AtCSLD2

To explore the location of AtCSLD proteins, we generated and characterized polyclonal antibodies directed against peptides derived from AtCSLD2 or -D3. Because the antibody against the AtCSLD3-specific peptide did not recognize a specific protein from *Arabidopsis* extracts under conditions of the strategy described below, we selected AtCSLD2 to represent the AtCSLD family for our studies.

To produce a polyclonal antibody that specifically recognized AtCSLD2, we used as antigen a short peptide of 18

aa from the N-terminus (the antigen peptide's position is indicated in Fig. 1). We performed affinity purification of the antibodies using immobilized antigenic peptide. To characterize the purified antibodies, we expressed in *Escherichia coli* a polypeptide fragment, P2, containing the N-terminal 272 amino acids from AtCSLD2 (Fig. 1); and a polypeptide fragment, P3, containing a similar region, the N-terminal 188 aa from AtCSLD3. Neither of the fragments contained any of the predicted transmembrane domains of the corresponding full-length proteins (see Fig. 1). The expression of P2 and P3 in *E. coli* was confirmed by SDS-PAGE followed by protein staining (Fig. 2a) and immunoblotting using antibodies against the 6× His tag (Fig. 2b). When tested on the *E. coli* extracts containing fragment P2 or P3, the peptide antibody against AtCSLD2 recognized only the expressed AtCSLD2 fragment P2 but not P3, which was derived from the equivalent region of AtCSLD3 (Fig. 2c). Because the AtCSLD3 protein is the closest homolog of the AtCSLD2 protein, we concluded that this antibody is specific for AtCSLD2. Other smaller proteins that were detected on the immunoblots were probably degradation products of P2 (Fig. 2c).

Three proteins were detected when the purified anti-D2-peptide antibodies were used to probe proteins from an *Arabidopsis* S10 fraction (Fig. 3a, signals 120, 90, and 30). All three signals disappeared when the purified antibodies were incubated with extracts from *E. coli* cells expressing fragment P2, before they were used for immunoblotting against *Arabidopsis* proteins. *E. coli* extracts containing fragment P3 did not show such an effect (data not shown); therefore, all three proteins (signals 120, 90, and 30) contained antigenic epitopes that can be recognized by the anti-peptide antibodies.

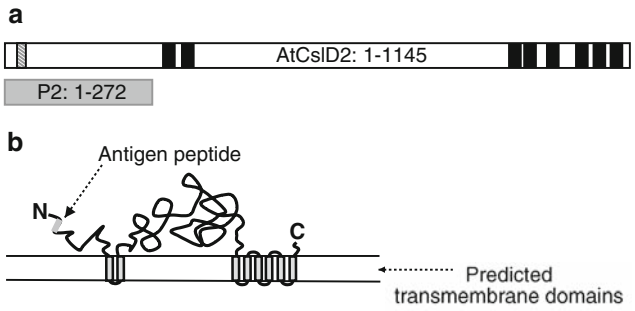

Fig. 1 AtCSLD2 protein. **a** Schematic diagram of the amino acid sequence (1–1145 aa) of AtCSLD2 (At5g16910). The *filled black boxes* represent the predicted eight transmembrane domains (located at amino acids 288–310, 323–341, 923–945, 952–974, 993–1015, 1046–1064, 1079–1097, 1110–1128). Peptide 20–36 (*small gray striped box*) was the antigen for producing antibodies. Peptide 1–272 (*large gray box* underneath) was expressed in *E. coli* with 6′His tag as P2. **b** The predicted topology of AtCSLD2 protein. Transmembrane domains (*bars* across the membrane) are predicted by the TMHMM server (http://www.cbs.dtu.dk/services/TMHMM/). The antigen peptide is depicted by the *small bar* close to the N-terminus

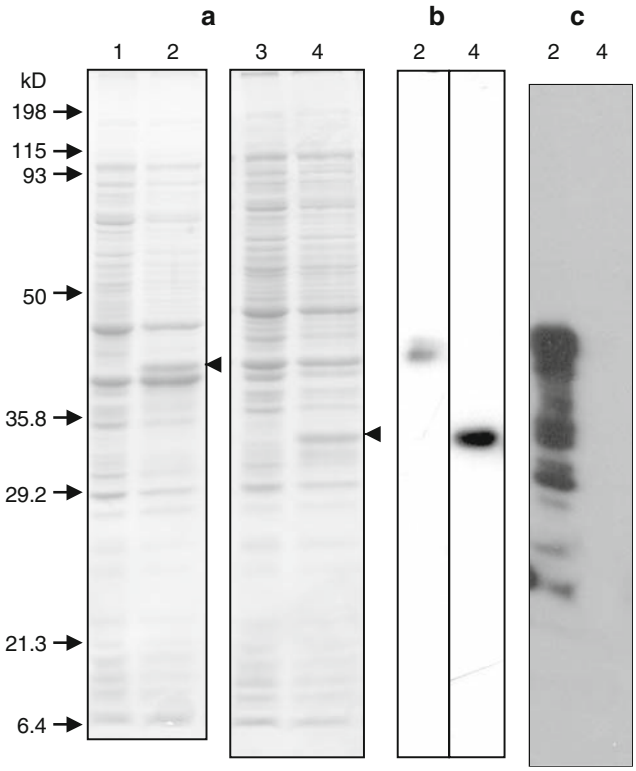

Fig. 2 Peptides P2 and P3 expressed in *E. coli* BL21 (DE3) cells. Equal amounts of protein extract from cells expressing peptide P2 (*lanes 1* and *2*) and P3 (*lanes 3* and *4*) were resolved on 12.5% SDS-PAGE. *Lanes 1* and *3*: total protein extracts before induction; *lanes 2* and *4*: total protein extracts after 3 h induction. Induced peptides P2 and P3 are indicated by *arrowheads*. **a**. Proteins stained with Coomassie Brilliant Blue. **b**. Immunoblots using antibodies against 6′His tag. **c**. Immunoblots using the antibodies against AtCSLD2. Aliquots of equal amounts were used in all three panels

When the S10 proteins were further fractionated into S100 (soluble) and P100 (microsomal membrane) fractions, signal 90 was mainly associated with the S100 fraction and therefore likely to be a soluble protein (Fig. 3a). Although both signals 120 and 30 were associated with the P100 fraction, only signal 120 was of the proper molecular size to represent AtCSLD2 (about 120 kD) (Fig. 3a). AtCSLD2 is predicted to have eight transmembrane domains (Fig. 1), and therefore should be an integral membrane protein. Because only signal 120 was associated with microsomal membranes and had a molecular mass similar to that predicted for AtCSLD2 (120 kD), we concluded that signal 120 likely represents AtCSLD2 proteins (Fig. 3). Furthermore, when vesicles enriched in Golgi membranes were prepared from *Arabidopsis* cell suspension cultures, only signal 120 was detected with the purified antibody against AtCSLD2 (Fig. 3b).

To find out what proteins signals 90 and 30 might represent, we searched the *Arabidopsis* protein sequence

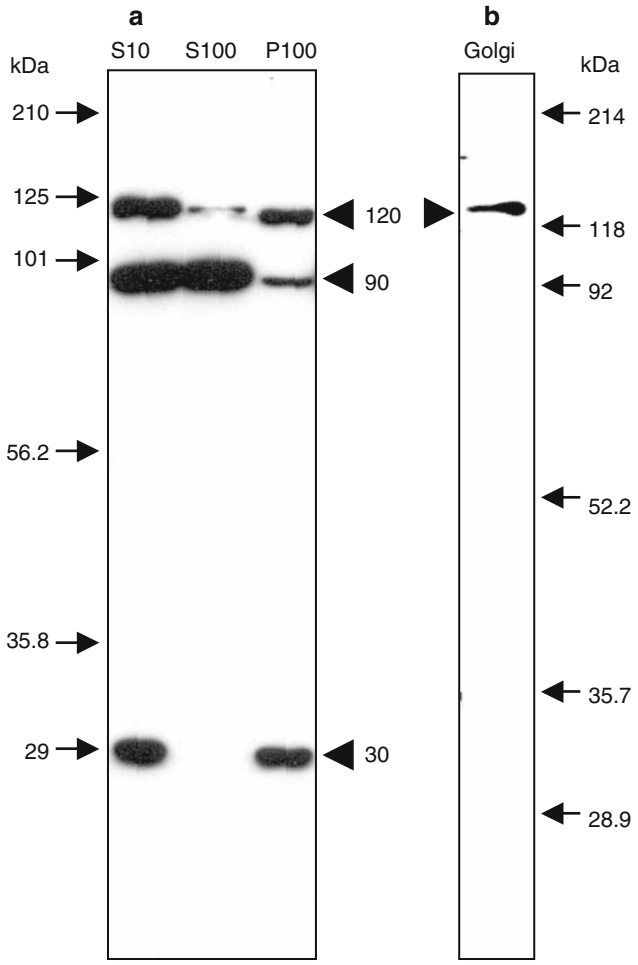

Fig. 3 Immunoblots using purified anti-D2-peptide antibodies against fractions from *Arabidopsis* extracts (**a**) and a Golgi complex-enriched fraction (**b**). **a** S10, S100, and P100 were extracted from freshly ground hydroponic plants. Immunoblot signals are marked as 120, 90, and 30 according to their estimated molecular mass. **b** Proteins from *Arabidopsis* vesicles enriched for Golgi membrane were used for SDS-PAGE and immunoblotting with the same antibodies. Golgi samples were prepared from suspension-cultured cells

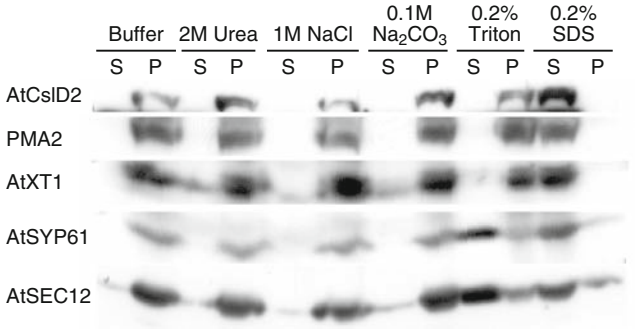

Fig. 4 AtCSLD2 is an integral membrane protein. Equal amounts of protein from P100 fraction prepared from hydroponically grown *Arabidopsis* plants were incubated on ice for 30 min with buffer alone, or with buffers containing 2 M Urea, 1 M NaCl, 0.1 M Na_2CO_3, 0.2% Triton X-100, or 0.2% SDS, and separated again as S100 and P100 fractions by centrifugation at 100,000g for 1 h. Pellets were resuspended in the same volume of buffer as the supernatant. Equal volumes of each fraction were analyzed by SDS-PAGE and immunoblotting was performed using antibodies against AtCSLD2, plasma membrane marker PMA2, Golgi markers XT1, TGN marker SYP61, and ER marker SEC12. *S* supernatant fractions; *P* pellet fractions

database at the National Center for Biotechnology Information (NCBI) using program BlastP searching for short nearly exact matches, with the sequence of the D2-specific antigen peptide as query. We identified ten proteins as having a region of two to six amino acids identical with the AtCSLD2-specific antigen peptide (data not shown). One of these ten proteins, which contained five sequential amino acids identical to the D2-specific antigen peptide, was predicted to have a molecular mass of 83 kD and no transmembrane domain. Another, with a stretch of four identical amino acids, was predicted to be 36 kD with a single transmembrane domain. No other proteins have a predicted molecular mass closer to that observed for signals 90 or 30. Although these two predicted proteins may give rise to the detected signals, we chose not to pursue this issue further.

AtCSLD2 is an integral membrane protein

As noted above, sequence analysis predicted that AtCSLD2 protein contains eight transmembrane domains (Fig. 1). After sequential centrifugation at 10,000*g* and at 100,000*g*, the majority of signal 120 was present in the P100 membrane fraction (Fig. 3a), indicating that signal 120, presumably representing AtCSLD2, was associated with membranes. To investigate whether the putative AtCSLD2 behaved as an integral membrane protein or as a peripheral membrane protein, we treated microsomal membranes from the P100 fraction with various reagents that affect the association of peripheral proteins with membranes (Fig. 4). Our results showed that the antigenic protein could not be removed from microsomal membranes by 2 M Urea, 1 M NaCl, 0.1 M Na_2CO_3, or 0.2% Triton X-100, all of which can dissociate peripheral membrane proteins. Only 0.2% SDS completely solubilized the antigenic protein from the microsomal membranes, indicating that the putative AtCSLD2 was an integral membrane protein (Fig. 4).

We monitored several control proteins in this experiment to determine whether the solubilization procedure would yield the expected results. PMA2 is a plasma membrane H^+-ATPase with multiple transmembrane domains and a predicted topology similar to AtCSLD2, with four transmembrane domains near the N-terminus and six close to the C-terminus (Morsomme et al. 1998). In our experiment, PMA2 was also removed only by 0.2% SDS and behaved just like AtCSLD2 (Fig. 4). *Arabidopsis* XyG xylosyltransferase 1 (XT1) is predicted to be a type II integral membrane protein (Faik et al. 2002). XT1 was completely

solubilized only by 0.2% SDS, but trace amounts were also solubilized by all the other reagents used, except with the buffer alone (Fig. 4). Thus, XT1 was also an integral membrane protein but it may not be as tightly associated with the membranes as are AtCSLD2 and PMA2. *Arabidopsis* SEC12 is an ER-associated integral membrane protein that can be removed from membranes only by ionic or nonionic detergents but not by other treatments such as urea, salt, or alkaline conditions (Bar-Peled and Raikhel 1997). The behavior of SEC12 (Fig. 4) was the same as observed before (Bar-Peled and Raikhel 1997) and this protein served as a valuable control here. SEC12 also demonstrated a weaker association with the membranes; in addition to nearly complete solubilization by 0.2% SDS, SEC12 was also largely solubilized by 0.2% Triton X-100. SYP61 is a trans-Golgi network (TGN) protein with a single transmembrane domain near its C-terminus (Sanderfoot et al. 2000). It also showed a weaker association with membranes when compared with AtCSLD2 or PMA2, as SYP61 was also removed from the membrane by 0.2% Triton X-100 (Fig. 4).

AtCSLD2 was not a plasma membrane protein, as revealed by two-phase partitioning

To localize AtCSLD2 to a specific cellular compartment, we used three different fractionation procedures. We first tried to determine whether AtCSLD2 was located at the plasma membrane. An aqueous two-phase partitioning method that enriches the plasma membrane in the upper phase and most other cellular membranes in the lower phase was employed with three consecutive partitioning steps (Fig. 5). The upper and lower phases from the third partitioning (U3 and L3, respectively) were analyzed for XyG fucosyltransferase (FUTase) and β-glucan synthase II (GS II) activity to confirm the effect of partitioning (Fig. 5a). U3 showed about fourfold higher specific activity of GS II than L3 (Fig. 5a), indicating that the upper phase was enriched for plasma membrane. At the same time, about three times higher specific activity of XyG FUTase was detected in L3 than in U3 (Fig. 5a), indicating an enrichment of Golgi vesicles in L3. All phases were then analyzed by immunoblotting to locate AtCSLD2 and the Golgi marker protein XT1, TGN marker protein SYP61, pre-vacuolar compartment (PVC) marker protein SYP21, TGN-PVC marker protein ELP, plasma membrane marker protein PMA2, and ER marker protein SEC12 (Fig. 5b). At the end of the third partitioning, AtCSLD2 was found primarily in the lower phase, which also contained markers derived from Golgi, TGN, PVC, and ER. Furthermore, we examined the marker proteins for mitochondria (alternative oxidase, AOX) and chloroplast (AtToc75), and found that they both were associated with the lower phase (data not shown). On the other hand, the plasma membrane marker PMA2, partitioned predominantly into the upper phase (Fig. 5b). From these observations, we concluded that AtCSLD2 was not localized in the plasma membrane.

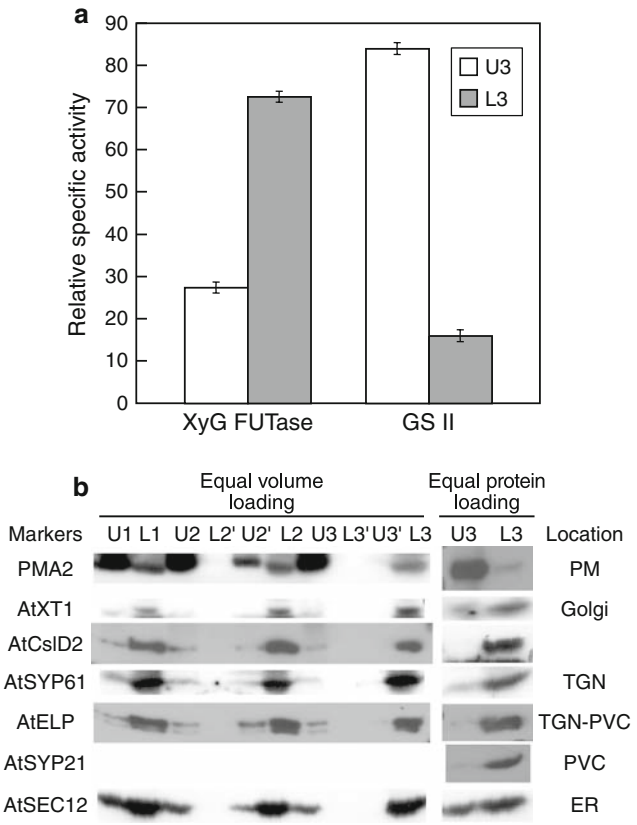

Fig. 5 Two-phase partitioning of *Arabidopsis* microsomal membranes (see "Materials and methods"). *U1* and *L1* fractions are the upper and lower phases after first partitioning. U2 and L2′, or U2′ and L2 are derived from the second partitioning of fractions U1 or L1, respectively. U3 and L3′, or U3′ and L3 were derived from the third partitioning of fractions U2 or L2, respectively. **a** Relative specific activity of GSII and XyG FUTase in fractions U3 (*white bars*) and L3 (*gray bars*). The absolute specific activity measurements showed differences between replicates, but the ratios of specific activity between U3 and L3 were always very similar. The graph shows the average ratio derived from three experiments with standard errors. **b** Aliquots of equal volume from each fraction were analyzed by SDS-PAGE and immunoblotting with antibodies against marker proteins PMA2 (plasma membrane), XT1 (Golgi), SYP61 (TGN), ELP (TGN-PVC), SYP21 (PVC) and SEC12 (ER). Equal amounts of protein were also taken from fractions U3 and L3 for similar analysis. Data shown here are from a single experiment with protein samples extracted from suspension-cultured cells. Two other independent experiments gave similar results

AtCSLD2 migrated differently from the plasma membrane marker but similar to Golgi markers during linear sucrose gradient centrifugation

Next we sought to determine which compartment within the endomembrane system contained AtCSLD2. Because of the similarity shared between AtCSLD and AtCESA

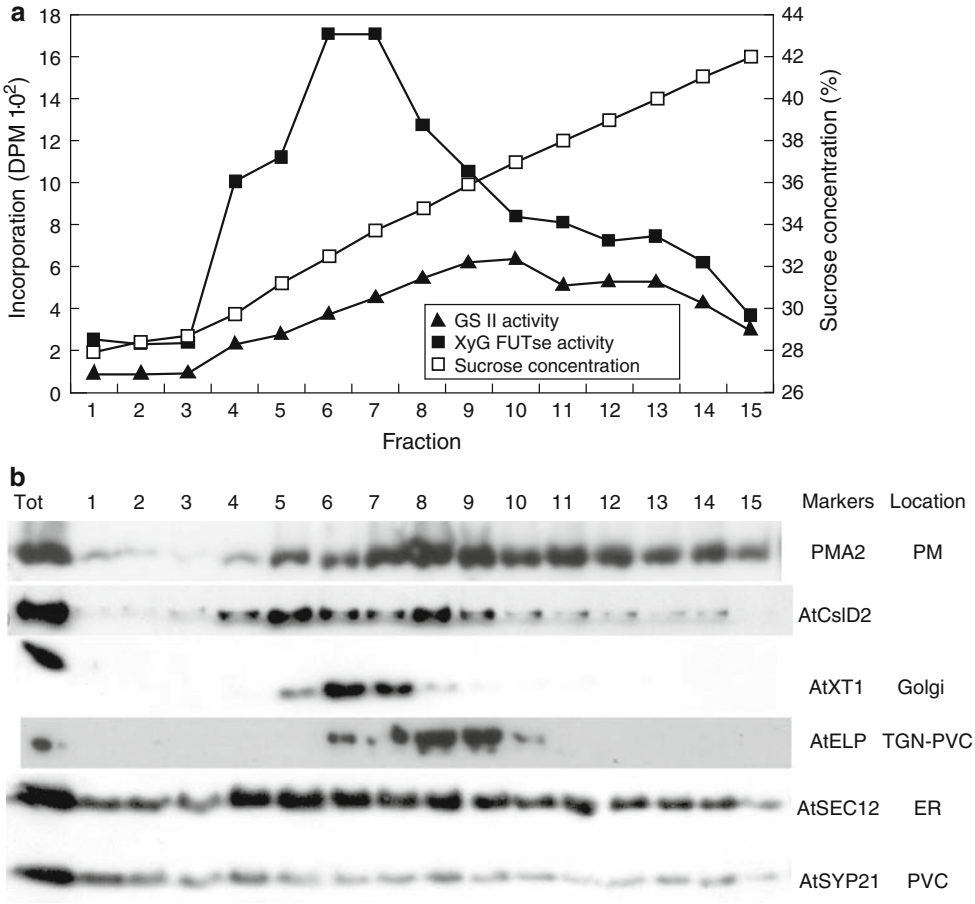

Fig. 6 Migration of AtCSLD2 and selected marker proteins on a linear sucrose density gradient (see "Materials and methods"). **a** Sucrose concentration and enzyme activities of XyG FUTase and GS II for each fraction of the linear sucrose gradient. **b** Immunodetection of AtCSLD2 and marker proteins PMA2 (plasma membrane), XT1 (Golgi), ELP (TGN-PVC), SEC12 (ER), and SYP21 (PVC). This particular experiment was repeated three times, with similar results each time. The dip in intensity of the AtCSLD2 protein observed in fractions 6 and 7 was not always seen, but this particular experiment is shown because the quality of other marker proteins is much better in this replicate

proteins, we believe that AtCSLD2 proteins are not likely to be located in mitochondria, plastids, or nuclei. As additional evidence against a nuclear localization, the elimination of nuclei during the first step of protein preparation for all experimental procedures (see "Materials and methods") did not significantly reduce the AtCSLD2 signal in subsequent immunoblots (Figs. 3, 4, 5, 6, 7, 9). Later on, when more refined membrane preparations were used and most plastids were removed due to their high density, a dramatic decrease or even total loss of signals was observed for chloroplast marker proteins Toc75 and Tic40 (data not shown). However, AtCSLD2 proteins could still be detected as before (Figs. 6, 7, 9), indicating that AtCSLD2 proteins are not likely to be located in plastid membranes.

Sedimentation centrifugation through a linear sucrose density gradient was employed in an attempt to resolve different membranes such as the ER, Golgi, PVC, and plasma membrane. As a first step of enrichment, crude microsomal membranes from *Arabidopsis* suspension-cultured cells were collected from the interface of a step gradient containing 15 and 50% sucrose. The membrane vesicles from the interface were recovered and further fractionated on a density gradient from 30 to 50% sucrose. After centrifugation, the sucrose density gradient was nearly linear (Fig. 6a). We analyzed the fractions using enzyme assays and immunoblots to detect marker enzymes that could help identify the vesicles derived from various organelles. XyG FUTase activity, a Golgi marker, peaked in fractions 6 and 7 (Fig. 6a). Immunoblotting demonstrated that XT1, another Golgi marker, was detected in the same fractions (Fig. 6b), leading to the conclusion that maximal enrichment of Golgi membranes was obtained in these fractions. AtCSLD2 was distributed most abundantly in fractions 4–9 (Fig. 6b), which overlaps with the Golgi markers XyG FUTase and XT1, but with a broader distribution. All of the other markers were significantly different from the pattern shown by AtCSLD2. The plasma membrane marker, PMA2, was broadly distributed throughout the gradient with a broad

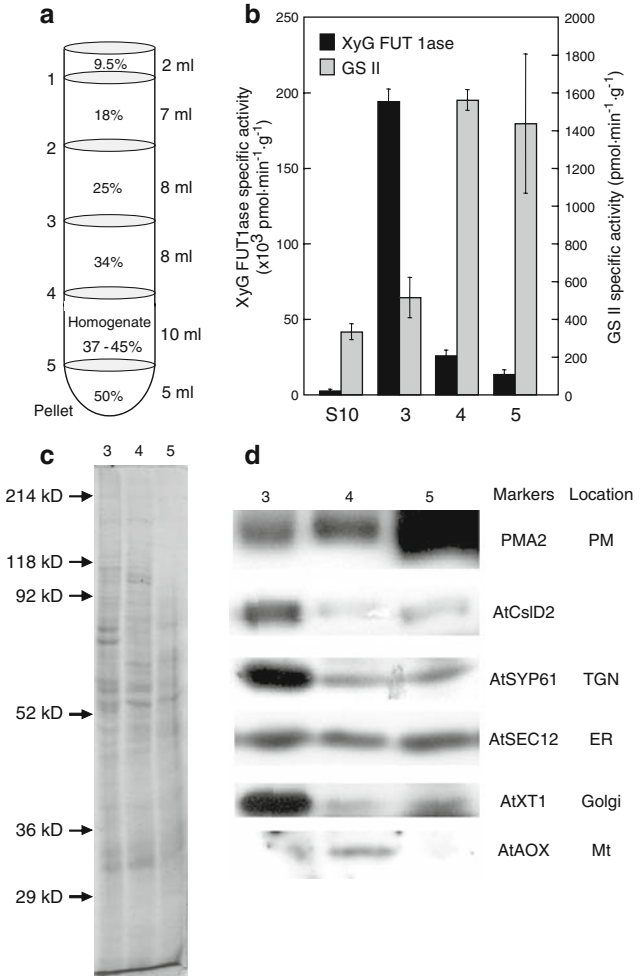

Fig. 7 Fractionation of microsomal vesicles by flotation centrifugation on a sucrose step gradient (see "Materials and methods"). The membranes present at the interfaces between different sucrose concentrations were collected as fractions *1–5* (**a**). Proteins from fractions *3*, *4* and *5*, as well as from the *S10* fraction starting material were assayed for XyG FUTase and GS II activities (**b**). Protein profiles of fractions *3*, *4*, and *5* were visualized by Coomassie Brilliant Blue staining with equal loading (13 mg) (**c**). Distribution of AtCSLD2 and marker proteins PMA2 (plasma membrane), SYP61 (TGN), SEC12 (ER), XT1 (Golgi), and alternative oxidase (AOX) (mitochondria) (**d**). Data shown in **b** are the average of three replicate experiments. Immunoblot shown in **d** is from a single experiment; two other independent replicate experiments gave similar results

peak area from fractions 7 to 14 (Fig. 6b). The distribution of PMA2 detected by immunoblot coincided relatively well with the pattern of the GSII activity distribution in the gradient (Fig. 6a). Meanwhile, the TGN-PVC marker ELP had the highest abundance in fractions 8 and 9, which was different from the distribution pattern of either AtCSLD2, or the Golgi markers XyG FUTase and XT1 (Fig. 6b). Finally, the PVC marker protein SYP21 and the ER marker SEC12 both had a broader distribution pattern that seemed to be a smear throughout the gradient (Fig. 6b). Repeated attempts to detect TGN marker SYP61 in linear sucrose gradients failed for reasons that we do not understand (data not shown). Therefore, it seemed that AtCSLD2 is more likely to be located at the Golgi instead of other endomembranes, but has a different distribution pattern through the Golgi cisternae than the XyG FUTase or XT1.

AtCSLD2 protein was localized in Golgi-rich vesicles during floatation sucrose gradient centrifugation

Because efforts to localize AtCSLD2 using linear sucrose gradients were not conclusive, we sought an independent approach to this problem. As a third method to investigate the localization of AtCSLD2, we isolated microsomal membranes from *Arabidopsis* suspension-cultured cells and fractionated via flotation on a sucrose step gradient (Fig. 7a). We evaluated the enrichment of Golgi and plasma membrane vesicles by performing XyG FUTase and GS II activity assays, respectively (Fig. 7b). The specific activity of XyG FUTase in the Golgi-rich fraction (fraction 3) was more than 75 times greater than that in the starting material (Fig. 7b). Fraction 5 was depleted in Golgi membrane; its specific activity for XyG FUTase was only about 7% of that in fraction 3. On the other hand, the GS II specific activity was similar in fractions 4 and 5 (Fig. 7b). The Golgi enriched membranes (fraction 3) showed some incorporation of radiolabeled glucose during GS II activity assays (Fig. 7b). However, the GSII activity recorded for fraction 3 may not reflect its true level because when reactions were carried out for 45 versus 15 min, the radiolabel incorporation did not increase as expected (data not shown). In contrast, during GSII assays with other fractions, the incorporation of radiolabeled glucose increased significantly when assayed for 45 min instead of 15 min (data not shown).

When equal amount of proteins from each fraction were used for immunoblots (Fig. 7c), we noticed that TGN marker protein SYP61 and Golgi marker protein XT1 were found almost exclusively in fraction 3 (Fig. 7d), whereas the plasma membrane marker protein PMA2 was detected mainly in fraction 5 (Fig. 7d), with small amounts in fractions 3 and 4. Taken together, these results supported the conclusion that fraction 3 was enriched in Golgi complex and fraction 5 was enriched in plasma membrane. Fraction 4, on the other hand, not only contained a mixture of these two membranes, but also was enriched in mitochondria, as demonstrated by the presence of the marker protein alternative oxidase (Fig. 7d). The majority of AtCSLD2 was detected in fraction 3 (Fig. 7d), leading us to conclude that AtCSLD2 was located in the Golgi-rich vesicles. Furthermore, the ER was distributed almost equally among fractions 3, 4 and 5, as revealed by the distribution pattern of ER marker protein SEC12 (Fig. 7d). From these observations, we concluded that AtCSLD2 was not likely located at the ER membrane. However, it was not possible to resolve

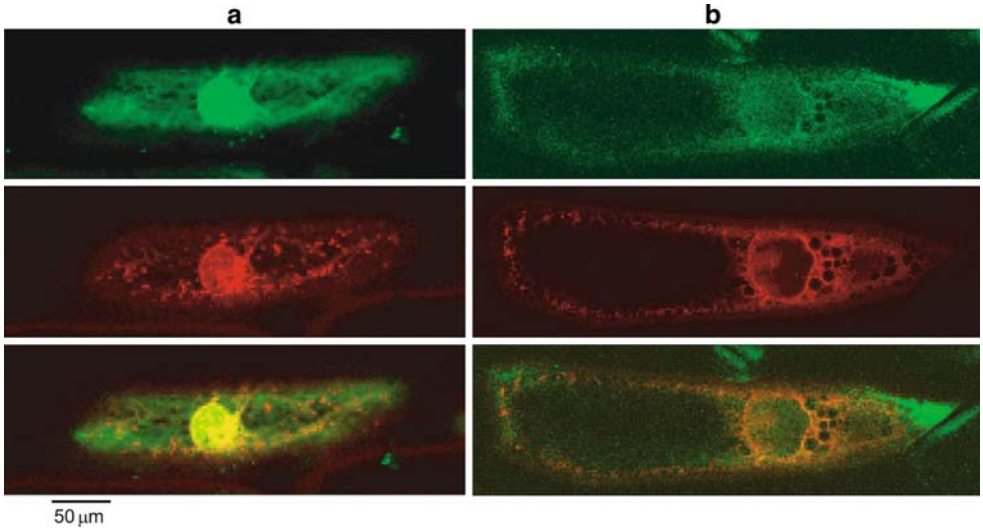

Fig. 8 When transiently expressed in onion epidermal cells, AtCSLD2-GFP fusion proteins are detected in the Golgi vesicles labeled by ST-DsRed. **a** Control coexpression of GFP protein alone together with ST-DsRed protein. **b** An onion epidermal cell coexpressing AtCSLD2-GFP fusion protein and ST-DsRed protein

Golgi and TGN using this procedure because the Golgi marker XT1 and the TGN marker SYP61 showed similar distribution patterns (Fig. 7d).

We noticed that one plasma membrane marker, the GSII activity, had an almost equal distribution between fractions 4 and 5 (Fig. 7b), whereas another plasma membrane marker, the PMA2 protein, was detected mainly in fraction 5 by immunoblotting (Fig. 7d). This observation may indicate the presence of multiple enzyme activities that catalyzed the polymerization of UDP-glucose and contributed to the readings recorded as GSII activity.

AtCSLD2-GFP colocalized with ST-DsRed at Golgi vesicles when transiently expressed in onion epidermal cells

To obtain a different line of evidence for the localization of AtCSLD2 proteins, we constructed a AtCSLD2-GFP fusion protein by replacing the predicted hydrophilic catalytic domain of AtCSLD2 (amino acids 381–889, Fig. 1) with an in-frame GFP protein while retaining all of the predicted transmembrane domains ("Materials and methods"). This fusion protein AtCSLD2-GFP was transiently expressed in onion epidermal cells together with a Golgi marker protein ST-DsRed (Saint-Jore et al. 2002). Confocal fluorescent microscopy showed that most of the signals from AtCSLD2-GFP proteins overlapped with signals from ST-DsRed located on Golgi vesicles (Fig. 8b). Meanwhile the GFP protein itself showed a very different localization pattern when coexpressed with ST-DsRed as control (Fig. 8a).

The AtCSLD2 N-terminus was not protected by the Golgi membrane during proteinase K treatment

To evaluate the topology of AtCSLD2 within the Golgi membrane, we used a proteinase K protection assay to determine availability of the N-terminus of AtCSLD2. Vesicles enriched in Golgi complex membranes were subjected to proteinase K treatment, then assayed for XyG FUTase activity and resolved on SDS-PAGE for immunoblotting. XyG FUTase activity is a latent Golgi activity because permeabilization of the Golgi membranes by detergent is required for measurement of its activity (Hanna et al. 1991; Wulff et al. 2000). Therefore, we used the XyG FUTase activity as a marker for the inside of the Golgi complex membrane.

We first used XyG FUTase activity assays to validate the intactness and orientation of the Golgi vesicle preparation during the proteinase K treatment protocols. By comparing the XyG FUTase activity levels from Golgi vesicles with or without including Triton X-100 in the enzyme activity assay reactions, we observed that greater than 90% of the activity was latent and therefore concluded that less than 10% of the Golgi vesicles were inside out or broken (data not shown). We determined that under our assay conditions proteinase K did not penetrate the Golgi membranes because enzyme treatment destroyed only a very small amount of XyG FUTase activity when the Golgi vesicles were not treated with Triton X-100 (Fig. 9a, reactions 2 and 3). On the other hand, when the Golgi vesicles were permeabilized with detergent prior to proteinase K treatment, almost all of the XyG FUTase activity was degraded (Fig. 9a, reactions 5 and 6). In addition to XyG FUTase, many other proteins were also protected from degradation when Golgi vesicles were not permeabilized during proteinase K treatment (Fig. 9b, reactions 2 and 3). Presumably, those proteins also face the inside of the Golgi vesicles. However, an almost complete degradation of the proteins was achieved when the Golgi vesicles were treated with Triton X-100 during proteinase K treatment (Fig. 9b, reactions 5 and 6).

Using the treatment conditions described above, we examined the presence of AtCSLD2 and XT1 by immunoblot

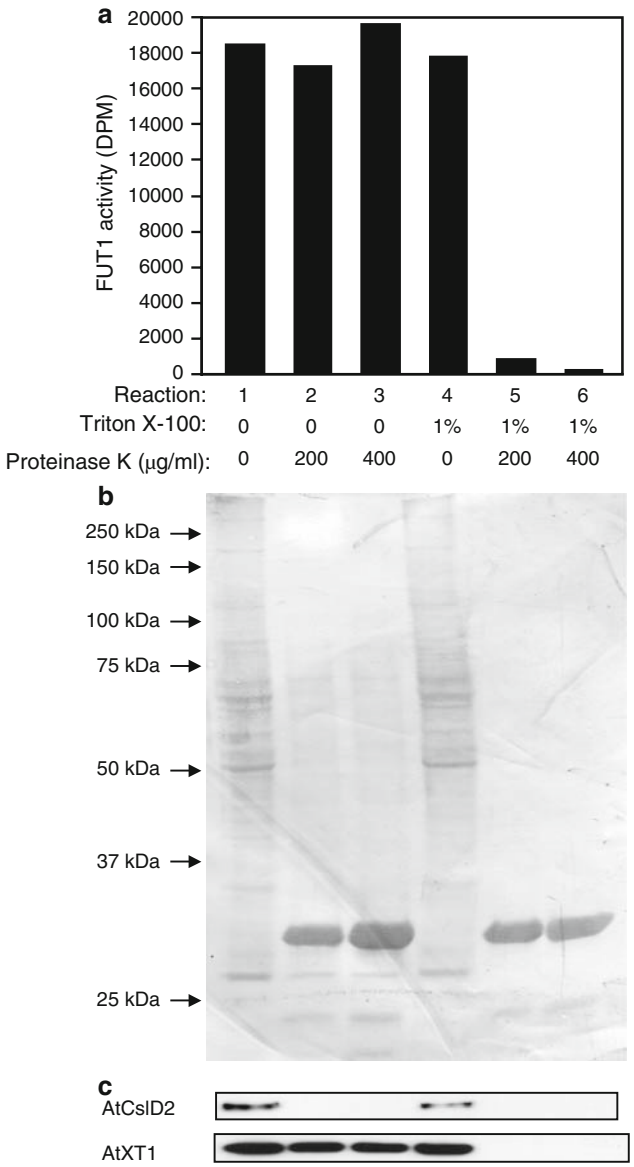

Fig. 9 AtCSLD2 is not protected by Golgi membranes during proteinase K treatment, whereas XT1 proteins and XyG FUTase activity are. The samples and reaction conditions are all the same in **a, b,** and **c**. Equal amounts of Golgi-rich vesicles were treated with 0 µg/ml (reactions *1* and *4*), 200 µg/ml (reactions *2* and *5*), or 400 µg/ml (reactions *3* and *6*) proteinase K with (reactions *4*, *5*, and *6*) or without (reactions *1*, *2*, and *3*) the presence of 1% Triton X-100. After treatment, equal amounts of samples were assayed for XyG FUTase activity in the presence of 1% Triton X-100 (**a**), visualized on SDS-PAGE with Coomassie Brilliant Blue staining (**b**), or subjected to immunoblot analysis with antibodies against XT1 and AtCSLD2 (**c**). Data shown are from a single experiment; two replicate experiments gave similar results. The percentage of inside-out Golgi complex vesicles is determined by comparing the XyG FUTase activity assayed with or without permeabilization of the membrane vesicles with 1% Triton X-100. In this case, the inside-out or unsealed vesicles constitute only 8.8% of the total

assay (Fig. 9c). Our earlier data (Figs. 4, 5, 6, 7) showed that XT1 was a Golgi-localized integral membrane protein, and we used this result as a control. XT1 is predicted to be a type II transmembrane protein with a single transmembrane domain near its N-terminus and facing the Golgi lumen (Faik et al. 2002). The antibody against XT1 used in this work was generated against the large domain after the N-terminal transmembrane domain (A. Faik and K. Keegstra, unpublished data). Therefore, if XT1 is facing the Golgi lumen, it should be protected from proteinase K when Golgi vesicles are not permeabilized. Indeed, we saw no change in signal intensity when Golgi vesicles were treated with proteinase K without the addition of Triton X-100 (Fig. 9c, reactions 2 and 3). However, when Triton X-100 was added to the Golgi vesicles, XT1 was completely degraded by proteinase K (Fig. 9c, reactions 5 and 6).

Immunoblot signals for AtCSLD2 showed a different pattern (Fig. 9c). AtCSLD2 was completely degraded by proteinase K treatment regardless of whether or not Triton X-100 was present in the reaction mixture (Fig. 9c, reactions 2, 3, 5, and 6). From this observation, we concluded that the antigenic region (the extreme N-terminus) of AtCSLD2 was located on the outer surface of the Golgi membrane, facing the cytosol. Alternatively, if the N-terminus of AtCSLD2 were inside the Golgi lumen, then the closest cleavage site accessible to proteinase K would have been right after the first transmembrane domain (Fig. 1). In this case, an AtCSLD2 peptide from amino acid residues 1 to 287 with a predicted molecular mass of around 32 kD should have been detected by our antibody as the degradation product. What we saw from the immunoblot, however, was a total disappearance of signal for the full-length AtCSLD2, and no appearance of new signals with smaller molecular mass (Fig. 9c).

The program TMHMM predicts that AtCSLD2 has eight transmembrane domains (Fig. 1): two are located between the N-terminal peptide used as antigen and the large hydrophilic domain (Fig. 1). If this prediction were correct, our data supported the conclusion that the large hydrophilic domain of AtCSLD2 faced the cytosol.

Discussion

Although genetic approaches have been used successfully to analyze the functions of many *AtCESA* genes (Arioli et al. 1998; Taylor et al. 1999, 2000; Fagard et al. 2000; Scheible et al. 2001; Burn et al. 2002; Desprez et al. 2002; Zhong et al. 2003) and some genes involved in the biosynthesis of matrix polysaccharides (Bouton et al. 2002; Iwai et al. 2002; Vanzin et al. 2002; Madson et al. 2003), genetic studies for *CSL* genes have not been as successful in determining their biochemical functions. So far, mutations in only a few *CSL* genes have yielded specific phenotypes, including *AtCSLA7* (Goubet et al. 2003), *AtCSLA9*/*rat4* (Zhu et al. 2003), *AtCSLD3*/*kojak (kjk)* (Favery et al. 2001;

Wang et al. 2001), *AtCSLD5* (Bernal et al. 2007), and *OsCSLD1*(Kim et al. 2007). However, none of the mutations have been linked to changes in specific sugar linkages within a specific cell wall polysaccharide and therefore the biochemical functions of these genes could not be determined from these studies. Furthermore, our attempt to suppress multiple *AtCSLD* genes using an RNAi approach did not yield changes in any specific sugar linkages (Zeng 2004). Therefore, we conducted localization and topological studies of AtCSLD proteins to find out whether this information would offer some hints about their biochemical functions.

In our present study, we used three different membrane fractionation procedures to monitor the behavior of AtCSLD2 proteins during cell fractionation. In the two-phase partitioning experiment, AtCSLD2 and the plasma membrane marker protein PMA2 were partitioned into different phases, which led us to conclude that AtCSLD2 is not located in the plasma membrane, but rather in some portion of the endomembrane system. Because AtCSLD2's distribution pattern in the linear sucrose density gradient is very different from the PVC marker protein SYP21, the TGN-PVC marker protein ELP, and the ER marker protein SEC12, we concluded that AtCSLD2 was not located in any of these fractions. On the other hand, the distribution pattern of AtCSLD2 matched best with that of Golgi marker protein XT1 and marker enzyme activity of XyG FUTase in all three membrane fractionation procedures (Figs. 5, 6, 7). Therefore, we concluded that AtCSLD2 most likely resides in the Golgi apparatus. We noted that the ER marker protein SEC12 was always detected within multiple membrane fractions (Figs. 5, 6, 7). This characteristic may indicate a physical closeness of the ER with other membrane compartments or the difficulty of separating ER membranes from other endomembranes with the techniques employed in our studies.

In addition to the cellular membrane fractionation approaches, the transient expression of AtCSLD2-GFP fusion protein in onion epidermal cells showed its localization in Golgi vesicles more directly. Bioinformatic tools helped to predict that AtCSLD2 proteins have eight transmembrane domains, with two of them located close to the N-terminus and the other six close to the C-terminus (Fig. 1). The region between these two groups of transmembrane domains of AtCSLD2 is the predicted catalytic domain. In our AtCSLD-GFP fusion protein, this catalytic domain was replaced by the GFP, with all the predicted transmembrane domains of AtCSLD2 kept intact. This design of GFP fusion protein therefore kept the relative positions of all the transmembrane domains similar to the endogenous AtCSLD2 proteins. The AtCSLD2-GFP fusion protein showed a localization pattern similar to a Golgi marker protein ST-DsRed, which has the transmembrane domain and the short cytoplasmic tail (52 amino acids) of the rat α-2,6-sialyltransferase (ST) fused with DsRed (BD Clontech) and was shown to localize at the Golgi apparatus (Brandizzi et al. 2002; Saint-Jore et al. 2002). Based on these results, we argue that AtCSLD2 proteins are most likely located in the Golgi. Our conclusion that AtCSLD2 was localized at the Golgi is consistent with Bernal et al.'s observation when they studied localization with N-terminal GFP fusion proteins of AtCSLD5 and AtCSLD3 (Bernal et al. 2007).

Another important question regarding glycosyltransferases and glycan synthases concerns their topology within the membrane. Most glycosyltransferases are thought to be type II membrane proteins with a single membrane-spanning domain and a large hydrophilic domain facing the lumen of the Golgi (Keegstra and Raikhel 2001). This topology has been experimentally demonstrated for the xyloglucan FUTase (Wulff et al. 2000), which was confirmed again in the studies reported here (Fig. 9). The substrate nucleotide sugars are proposed to be imported into the Golgi lumen by specific transporters, with the products accumulating in the Golgi lumen (Munoz et al. 1996; Neckelmann and Orellana 1998; Wulff et al. 2000; Sterling et al. 2001).

The topology of glycan synthases is a more complicated issue because of the presence of multiple transmembrane domains. It is widely accepted that cellulose synthase contains eight transmembrane domains that span the plasma membrane, and a large hydrophilic domain residing in the cytosol that presumably contains the active site (Delmer 1999). In this case, cellulose accumulates on the outside of the plasma membrane, indicating that cellulose synthase acts not only as a polymerase, but also as a transporter. However, the exact topology of the CESA protein has not yet been confirmed experimentally. Similarly, computer calculations predict the existence of multiple transmembrane domains in all of the CSL proteins (Richmond and Somerville 2000; Zeng 2004). CSLD, which has extensive sequence similarity to the CESA proteins, is predicted to have eight transmembrane domains by most of the on-line computer-based transmembrane domain prediction algorithms (Fig. 1). However, its topology within the membrane remains unclear.

The large hydrophilic domain of AtCSLD proteins, which is proposed to contain the catalytic activity of the enzyme, may face either the cytosol or the Golgi lumen. If the first case is true, the enzyme would function like cellulose synthase, using nucleotide sugars directly from the cytosol; and the polysaccharide product would be deposited on the other side of the membrane. If the second case is true, sugar nucleotides would be used in the lumen where the polysaccharide product accumulates; and transmembrane transport would be unnecessary (Scheible and Pauly 2004).

Prior to our studies reported here, the only similar topology study was carried out on the maize mixed linkage (1–3), (1–4)-β-glucan synthase (Urbanowicz et al. 2004). In that study, the pretreatment of Golgi membranes with increasing concentrations of proteinase K decreased the (1–3),(1–4)- β-glucan synthase activity accordingly. The catalytic domain of the (1–3),(1–4)- β-glucan synthase was thus proposed to be on the cytoplasmic face of the Golgi membranes, with extrusion of the growing polymer into the lumen of the Golgi. Therefore, topologically, the (1–3), (1–4)- β-glucan synthase behaves similarly to cellulose synthase.

In the topological study reported here, the N-terminus of AtCSLD2 was extremely sensitive to proteinase K treatment, regardless of whether or not Golgi vesicles were pretreated with Triton X-100. In contrast, both the XT1 protein and XyG FUTase activity were resistant to proteinase K treatment unless the Golgi vesicles were pretreated with Triton X-100. As noted above, using the program TMHMM, AtCSLD2 is predicted to have eight transmembrane domains, with two of them close to the N-terminus and the other six close to the C-terminus (Fig. 1). Based on these results and the transmembrane domain predictions, we concluded that the N-terminus of AtCSLD2 faces the cytosolic side of Golgi complex membranes. Using the membrane topology model of AtCSLD2 shown in Fig. 1, we deduced that the large hydrophilic loop containing the D,D,D,Q××RW motif also faces the cytosol. If correct, this conclusion would put AtCSLD2 into the same category topologically as the maize (1–3),(1–4)- β-glucan synthase and cellulose synthases, in regard to the mechanisms involved in the synthesis of respective polysaccharides.

The conclusion that the large hydrophilic loop containing the putative catalytic domain faces the cytosol is dependent upon a few assumptions that are relatively safe, but should be noted. The first is that the membrane vesicles are sealed so that in the absence of detergent, the protease cannot gain access to the lumen of the vesicles. Because both the XT1 protein and XyG FUTase activity are resistant to protease digestion in the absence of detergent, it seems reasonable to assume that the vesicles are sealed. The second assumption relates to the model that predicts the number and location of the putative transmembrane domains. The program used here, TMHMM, is normally very reliable in predicting the location of transmembrane domains (Krogh et al. 2001). In addition, when AtCSLD2 was analyzed for topology prediction by 17 different programs at Aramemnon (http://aramemnon.botanik.uni-koeln.de/index.ep), 14 of them, including TMHMM and the consensus predictions, gave the same topology as that shown in Fig. 1. Thus, the assumption regarding the transmembrane domain structure seems well supported, and it is reasonable to conclude that the N-terminus and the large hydrophilic domain of AtCSLD2 are on the same side of the membrane, i.e., the cytosolic side.

In summary, our data support the notion that AtCSLD2 is located at the Golgi membrane, but has a topology similar to cellulose synthase with the catalytic domain facing the cytoplasmic side of the Golgi. Nevertheless, we are still not able to predict the biochemical functions of AtCSLD proteins. On one hand, AtCSLD2 is located at the Golgi apparatus, based on the conventional concepts, and so likely functions as a non-cellulosic glycan synthase. Cellulose is believed to be synthesized at the plasma membrane and is directly incorporated into the wall, whereas the other polysaccharides are synthesized at the Golgi apparatus (Kimura et al. 1999). Likewise, cellulose synthases have long been thought to be exclusively localized at the plasma membrane and other glycan synthases and glycosyltransferases are thought to be located in the Golgi.

On the other hand, very recent localization studies on KORRIGAN1, an endo-1,4-β-D-glucanase involved in cellulose synthesis, and AtCSLA6, suggest that cellulose synthases might not reside exclusively in the plasma membranes, but rather commute between the plasma membranes and endomembranes, including Golgi vesicles (Robert et al. 2005; Paredez et al. 2006). Based on these observations and the Golgi localization of AtCSLD2 proteins shown by our study, a non-cellulosic function for AtCSLD proteins seems likely. However, because we did not explore the possibility of AtCSLD2 trafficking between Golgi and plasma membranes, we cannot rule out the possibility that our data represented no more than a small snapshot of the cellular distribution of AtCSLD2 proteins. Given different physiological conditions, AtCSLD2 proteins might distribute differently among different cellular compartments.

Acknowledgments This work was supported in part by a grant from the Plant Genome Program at the US National Science Foundation and in part by a grant from the Biosciences Program at the US Department of Energy. The authors thank Ahmed Faik for the gift of an antibody directed against AtXT1, Teruko Konishi for technical help during the development of the sucrose step gradient protocol, Shuocheng Zhang for help with transient expression in onion epidermal cells, Melinda K Frame for help with confocal microscopy, and Karen Bird for editorial assistance during the preparation of the manuscript.

References

Ahmed SU, Bar-Peled M, Raikhel NV (1997) Cloning and subcellular location of an *Arabidopsis* receptor-like protein that shares common features with protein-sorting receptors of eukaryotic cells. Plant Physiol 114:325–336

Arioli T, Peng L, Betzner AS, Burn J, Wittke W, Herth W, Camilleri C, Hofte H, Plazinski J, Birch R (1998) Molecular analysis of cellulose biosynthesis in *Arabidopsis*. Science 279:717–720

Axelos M, Curie C, Mazzolini L, Bardet C, Lescure B (1992) A protocol for transient gene expression in *Arabidopsis thaliana* protoplasts isolated from cell-suspension cultures. Plant Physiol Biochem 30:123–128

Bar-Peled M, Raikhel NV (1997) Characterization of AtSEC12 and AtSAR1. Plant Physiol 114:315–324

Bernal AJ, Jensen JK, Harholt J, Sorensen S, Moller I, Blaukopf C, Johansen B, de Lotto R, Pauly M, Scheller HV, Willats WGT (2007) Disruption of ATCSLD5 results in reduced growth, reduced xylan and homogalacturonan synthase activity and altered xylan occurrence in *Arabidopsis*. Plant J 52:791–802

Bouton S, Leboeuf E, Mouille G, Leydecker M-T, Talbotec J, Granier F, Lahaye M, Hofte H, Truong H-N (2002) *QUASIMODO1* encodes a putative membrane-bound glycosyltransferase required for normal pectin synthesis and cell adhesion in *Arabidopsis*. Plant Cell 14:2577–2590

Brandizzi F, Fricker M, Hawes C (2002) A greener world: the revolution in plant bioimaging. Nat Rev Mol Cell Biol 3:520–530

Buckeridge MS, Vergara CE, Carpita NC (1999) The mechanism of synthesis of a mixed-linkage (1–3),(1–4)β-D-glucan in maize. Evidence for multiple sites of glucosyl transfer in the synthase complex. Plant Physiol 120:1105–1116

Burn J, Hocart CH, Birch RJ, Cork AC, Williamson RE (2002) Functional analysis of the cellulose synthase genes *CesA1, CesA2, CesA3* in *Arabidopsis*. Plant Physiol 129:797–807

Campbell JA, Davies GJ, Bulone V, Henrissat B (1997) A classification of nucleotide-diphospho-sugar glycosyltransferases based on amino acid sequence similarities. Biochem J 326:929–939

Delmer D (1999) Cellulose biosynthesis: exciting times for a difficult field of study. Annu Rev Plant Physiol 50:245–276

Delmer DP, Stone BA (1988) Biosynthesis of plant cell walls. In: Priess J (ed) The biochemistry of plants. Academic Press Inc., New York, pp 373–421

Desprez T, Vernhettes S, Fagard M, Refregier G, Desnos T, Aletti E, Py N, Pelletier S, Hofte H (2002) Resistance against herbicide isoxaben and cellulose deficiency caused by distinct mutations in same cellulose synthase isoform CESA6. Plant Physiol 128:482–490

Dunkley TPJ, Hester S, Shadforth IP, Runions J, Weimar T, Hanton SL, Griffin JL, Bessant C, Brandizzi F, Hawes C, Watson RB, Dupree P, Lilley KS (2006) Mapping the *Arabidopsis* organelle proteome. Proc Natl Acad Sci USA 143:6518–8623

Elthon TE, Nickels RL, McIntosh L (1988) Monoclonal antibodies to the alternative oxidase of higher plant mitochondria. Plant Physiol 89:1311–1317

Fagard M, Desnos T, Desprez T, Goubet F, Refregier G, Mouille G, McCann M, Rayon C, Vernhettes S, Hofte H (2000) *PROCUSTE1* encodes a cellulose synthase required for normal cell elongation specifically in roots and dark-grown hypocotyls of *Arabidopsis*. Plant Cell 12:2409–2432

Faik A, Price NJ, Raikhel NV, Keegstra K (2002) An Arabidopsis gene encoding an alpha-xylosyltransferase involved in xyloglucan biosynthesis. Proc Natl Acad Sci USA 99:7797–7802

Favery B, Ryan E, Foreman J, Linstead P, Boudonck K, Steer M, Shaw P, Dolan L (2001) *KOJAK* encodes a cellulose synthase-like protein required for root hair cell morphogenesis in *Arabidopsis*. Genes Dev 15:79–89

Geshi N, Jorgensen B, Ulvskov P (2004) Subcellular localization and topology of beta (1, 4) galactosyltransferase that elongates beta (1, 4) galactan side chains in rhamnogalacturonan I in potato. Planta 218:862–868

Gibeaut DM, Hulett J, Cramer GR, Seemann JR (1997) Maximal biomass of *Arabidopsis thaliana* using a simple, low-maintenance hydroponic method and favorable environmental conditions. Plant Physiol 115:317–319

Goubet F, Misrahi A, Park SK, Zhang Z, Twell D, Dupree P (2003) AtCSLA7, a cellulose synthase-like putative glycosyltransferase, is important for pollen tube growth and embryogenesis in *Arabidopsis*. Plant Physiol 131:547–557

Hanna R, Brummell DA, Camirand A, Hensel A, Russell EF, Maclachlan GA (1991) Solubilization and properties of GDP-fucose xyloglucan 1, 2-alpha-L-fucosyltransferase from pea epicotyl membranes. Arch Biochem Biophys 290:7–13

Hanton SL, Chatre L, Renna L, Matheson LA, Brandizzi F (2007) De Novo formation of plant endoplasmic reticulum export sites is membrane cargo induced and signal mediated. Plant Physiol 143:1640–1650

Harlow E, Lane D (1988) Antibodies: a laboratory manual. Cold Spring Harbor Laboratory Press, Cold Spring Harbor, pp 498

Iwai H, Masaoka N, Ishii T, Satoh S (2002) A pectin glucuronyltransferase gene is essential for intercellular attachment in the plant meristem. Proc Natl Acad Sci USA 99:16319–16324

Keegstra K, Raikhel NV (2001) Plant glycosyltransferases. Curr Opin Plant Biol 4:219–224

Kim CM, Park SH, Je BI, Park SH, Park SJ, Piao HL, Eun MY, Dolan L, Han C-d (2007) OsCSLD1, a cellulose synthase-like D1 gene, is required for root hair morphogenesis in rice. Plant Physiol 143:1220–1230

Kimura S, Laosinchai W, Itoh T, Cui X, Linder CR, Brown RMJ (1999) Immunogold labeling of rosette terminal cellulose-synthesizing complexes in the vascular plant *Vigna angularis*. Plant Cell 11:2075–2085

Konishi T, Nakai T, Sakai F, Hayashi T (2001) Formation of callose from sucrose in cotton fiber microsomal membranes. J Wood Sci 47:331–335

Krogh A, Larsson B, von Heijne G, Sonnhammer ELL (2001) Predicting transmembrane protein topology with a hidden Markov model: application to complet genomes. J Mol Biol 305:567–580

Larsson C, Widell S, Kjellbom P (1987) Preparation of high-purity plasma membranes. Methods Enzymol 148:558–568

Liepman AH, Wilkerson CG, Keegstra K (2005) Expression of cellulose synthase-like (Csl) genes in insect cells reveals that CslA family members encode mannan synthases. Proc Natl Acad Sci USA 102:2221–2226

Madson M, Dunand C, Li X, Verma R, Vanzin GF, Caplan J, Shoue DA, Carpita NC, Reiter W-D (2003) The *MUR3* gene of Arabidopsis encodes a xyloglucan galactosyltransferase that is evolutionarily related to animal exostosins. Plant Cell 15:1662–1670

Morsomme P, Dambly S, Maudoux O, Boutry M (1998) Single point mutations distributed in 10 soluble and membrane regions of the *Nicotiana plumbaginifolia* plasma membrane PMA2 H+-ATPase activate the enzyme and modify the structure of the C-terminal region. J Biol Chem 273:34837–34842

Munoz P, Norambuena L, Orellana A (1996) Evidence for a UDP-glucose transporter in Golgi apparatus-derived vesicles from pea and its possible role in polysaccharide biosynthesis. Plant Physiol 112:1585–1594

Neckelmann G, Orellana A (1998) Metabolism of uridine 5′-diphosphate-glucose in Golgi vesicles from pea stems. Plant Physiol 117:1007–1014

Norambuena L, Marchant L, Berninsone P, Hirschberg CB, Silva H, Orellana A (2002) Transport of UDP-galactose in plants, identification and functional characterization of AtUTR1, an *Arabidopsis thaliana* UDP-galactose/UDP-glucose transporter. J Biol Chem 277:32923–32929

Northcote DH, Pickett-Heaps JD (1966) A function of the Golgi apparatus in polysaccharide synthesis and transport in the root-cap cells of wheat. Biochem J 98:159–167

Paredez AR, Somerville CR, Ehrhardt DW (2006) Visualization of cellulose synthase demonstrates functional association with microtubules. Science 312:1491–1495

Richmond TA, Somerville CR (2000) The cellulose synthase superfamily. Plant Physiol 124:495–498

Richmond TA, Somerville CR (2001) Integrative approaches to determining Csl function. Plant Mol Biol 47:131–143

Robert S, Bichet A, Grandjean O, Kierzkowski D, Satiat-Jeunemaitre B, Pelletier S, Hauser M-T, Hofte H, Vernhettes S (2005) An *Arabidopsis* endo-1, 4-beta-D-glucanase involved in cellulose synthesis undergoes regulated intracellular cycling. Plant Cell 17:3378–3389

Saint-Jore CM, Evins J, Batoko H, Brandizzi F, Moore I, Hawes C (2002) Redistribution of membrane proteins between the Golgi apparatus and endoplasmic reticulum in plants is reversible and not dependent on cytoskeletal networks. Plant J 29:661–678

Sanderfoot AA, Kovaleva V, Zheng H, Raikhel NV (1999) The t-SNARE AtVAM3p resides on the prevacuolar compartment in *Arabidopsis* root cells. Plant Physiol 121:929–938

Sanderfoot AA, Assaad FF, Raikhel NV (2000) The *Arabidopsis* genome. an abundance of soluble *N*-ethylmaleimide-sensitive factor adaptor protein receptors. Plant Physiol 124:1558–1569

Saxena IM, Brown RMJ, Fevre M, Geremia RA, Henrissat B (1995) Multidomain architecture of beta-glycosyltransferases: implications for mechanism of action. J Bacteriol 177:1419–1424

Scheible W-R, Eshed R, Richmond TA, Delmer D, Somerville CR (2001) Modifications of cellulose synthase confer resistance to isoxaben and thiazolidinone herbicides in *Arabidopsis Ixr1* mutants. Proc Natl Acad Sci USA 98:10079–10084

Scheible W-R, Pauly M (2004) Glycosyltransferases and cell wall biosynthesis: novel players and insights. Curr Opin Plant Biol 7:285–295

Sterling JD, Quigley HF, Orellana A, Mohnen D (2001) The catalytic site of the pectin biosynthetic enzyme alpha-1, 4-galacturonosyltransferase is located in the lumen of the Golgi. Plant Physiol 127:360–371

Taylor NG, Scheible W-R, Cutler S, Somerville CR, Turner SR (1999) The irregular xylem3 locus of *Arabidopsis* encodes a cellulose synthase required for secondary cell wall synthesis. Plant Cell 11:769–779

Taylor NG, Laurie S, Turner SR (2000) Multiple cellulose synthase catalytic subunits are required for cellulose synthesis in *Arabidopsis*. Plant Cell 12:2529–2539

Urbanowicz BR, Rayon C, Carpita NC (2004) Topology of the maize mixed linkage (1–3),(1–4)-beta-D-glucan synthase at the Golgi membrane. Plant Physiol 134:758–768

Vanzin GF, Madson M, Carpita NC, Raikhel NV, Keegstra K, Reiter WD (2002) The *mur2* mutant of *Arabidopsis thaliana* lacks fucosylated xyloglucan because of a lesion in fucosyltransferase AtFUT1. Proc Natl Acad Sci USA 99:3340–3345

Wang X, Cnops G, Vanderhaeghen R, Block SD, Montagu MV, Lijsebettens MV (2001) *AtCSLD3*, a cellulose synthase-like gene important for root hair growth in *Arabidopsis*. Plant Physiol 126:575–586

White AR, Xin Y, Pezeshk V (1993) Xyloglucan glucosyltransferase in Golgi membranes from *Pisum sativum* (pea). Biochem J 294:231–238

Wulff C, Norambuena L, Orellana A (2000) GDP-fucose uptake into the Golgi apparatus during xyloglucan biosynthesis requires the activity of a transporter-like protein other than the UDP-glucose transporter. Plant Physiol 122:867–877

Zeng W (2004) Xyloglucan biosynthesis: identification and characterization of fucosyltransferase and cellulose synthase-like genes. Cell and Molecular Biology Program, Michigan State University, East Lansing, Michigan

Zhang GF, Staehelin LA (1992) Functional compartmentation of the Golgi apparatus of plant cells: immunocytochemical analysis of high-pressure frozen and freeze-substituted sycamore maple suspension culture cells. Plant Physiol 99:1070–1083

Zhang SC, Wege C, Jeske H (2001) Movement proteins (BC1 and BV1) of Abutilon mosaic geminivirus are contransported in and between cells of sink but not a source leaves as detected by green fluorescent protein tagging. Virology 290:249–260

Zhong R, Morrison WHIII, Freshour GD, Hahn MG, Ye Z-H (2003) Expression of a mutant form of cellulose synthase AtCesA7 causes dominant negative effect on cellulose biosynthesis. Plant Physiol 132:786–795

Zhu Y, Nam J, Humara JM, Mysore KS, Lee LY, Cao H, Valentine L, Li J, Kaiser AD, Kopecky AL, Hwang HH, Bhattacharjee S, Rao PK, Tzfira T, Rajagopal J, Yi H, Veena, Yadav BS, Crane YM, Lin K, Larcher Y, Gelvin MJ, Knue M, Ramos C, Zhao X, Davis SJ, Kim SI, Ranjith-Kumar CT, Choi YJ, Hallan VK, Chattopadhyay S, Sui X, Ziemienowicz A, Matthysse AG, Citovsky V, Hohn B, Gelvin SB (2003) Identification of Arabidopsis *rat* mutants. Plant Physiol. 132: 494–505